Available online at www.sciencedirect.com

ScienceDirect

journal homepage: www.elsevier.com/locate/he

Laminar burning velocity of lean H_2–CO mixtures at elevated pressure using the heat flux method

M. Goswami [a,*], R.J.M. Bastiaans [a], A.A. Konnov [b], L.P.H. de Goey [a]

[a] Combustion Technology Section, Mechanical Engineering, Eindhoven University of Technology, 5612AZ Eindhoven, The Netherlands

[b] Division of Combustion Physics, Lund University, Lund, Sweden

ARTICLE INFO

Article history:
Received 20 September 2013
Received in revised form
28 October 2013
Accepted 31 October 2013
Available online 4 December 2013

Keywords:
Syngas
Laminar burning velocity
Heat flux method
Elevated pressure

ABSTRACT

Laminar burning velocity measurements of 50:50 and 85:15% (by volume) H_2–CO mixtures with O_2–N_2 and O_2–He oxidizers were performed at lean conditions (equivalence ratio from 0.5 to 1) and elevated pressures (1 atm–9 atm). The heat flux method (HFM) is employed for determining the laminar burning velocity of the fuel–oxidizer mixtures. HFM creates a one-dimensional adiabatic stretchless flame which is an important prerequisite in defining the laminar burning velocity. This technique is based on balancing the heat loss from the flame to the burner with heat gain to the unburnt gas mixture, in a very simple way, such that no net heat loss to the burner is obtained. Instabilities are observed in lean H_2–CO flames with nitrogen as the bath gas for pressures above 4 atm. Stable flames are obtained with helium as the bath gas for the entire pressure range. With the aim to cater stringent conditions for combustion systems such as gas turbines, an updated H_2–CO kinetic mechanism is proposed and validated against experimental results. The scheme was updated with recent rate constants proposed in literature to suit both atmospheric and elevated pressures. The proposed kinetic model agrees with new experimental results. At conditions of high pressure and lean combustion, reactions $H + O_2 = OH + O$ and $H + O_2 (+M) = H_2 (+M)$ compete the most when compared to other reactions. Reaction $H + HO_2 = OH + OH$ contributes to OH production, however, less at high-pressure conditions. At higher CO concentrations and leaner mixtures an important role of reaction $CO + OH = CO_2 + H$ is observed in the oxidation of CO.

1. Introduction

Renewed interest in the combustion characteristics of H_2–CO mixtures is motivated by the foreseeable increasing application of synthesis gas (syngas) in energy production and propulsion [1]. The integrated gasification combined cycle (IGCC) is one of the most recent technologies that utilize syngas to reduce NO_x emissions without compromising efficiency in power production. IGCC enables the conversion of coal and biomass to a gaseous synthetic fuel gas (syngas) in the gasifier. Syngas is a mixture of hydrogen (H_2), carbon monoxide (CO), carbon dioxide (CO_2) and steam (H_2O). In combination with gasification, removal of CO_2 is possible leaving increased levels of H_2. This technology of carbon capture and storage (CCS) is considered to be very promising. Usage of high hydrogen

* *Corresponding author*. Tel.: +31 402472877.
E-mail addresses: mayuri.goswami@gmail.com, m.goswami@tue.nl (M. Goswami).

0360-3199/$ – see front matter
http://dx.doi.org/10.1016/j.ijhydene.2013.10.164

content syngas may not only reduce the production of certain pollutants, it also increases the scope of utilizing its high energy content in the form of a fuel. Use of high H_2 fractions in combination with other gases like CO is a present trend that requires a great deal of research. Gas turbines used in such technology operate at conditions of high pressure, temperature and lean fuel–air mixtures. Hence, studying syngas combustion behavior at such conditions has become important.

The laminar burning velocity (S_L) defines the rate at which the unburnt mixture is consumed in a propagating laminar flame. This parameter is considered one of the most important entities in assessing many phenomena like flame quenching, flashback and stabilization in burners and combustors. Along with its importance in designing combustors for the systems mentioned above, this parameter also plays a key role in validating chemical reaction mechanisms. In theory, S_L can be obtained when a flame is one-dimensional, adiabatic and stretchless. There are a number of methods that can be employed to measure this quantity. Some of them are the counterflow flame method [2], spherically propagating flame method [3,4] and conical flame method [1]. The heat flux method (HFM) [5] is a relatively new method and has proven to be accurate for measuring S_L since it creates a flame very close to the one-dimensional, adiabatic and stretchless state. The main principle of the heat flux method is the stabilization of a flat flame with an unburnt gas velocity such that the heat loss by the flame needed to stabilize it on the burner is compensated by the heat added to the unburnt gases. This differential heat flux is reflected in the burner plate temperature profile that specifies the adiabatic state of the flame. In the present study, the end goal is to develop an improved kinetic mechanism that is appropriate in predicting lean syngas combustion at high pressure. In doing so, such a mechanism will be validated against experimental results obtained by the heat flux method and by other experiments from the literature.

Experimental data (S_L) for lean syngas/H_2-rich syngas mixtures at elevated pressure are scarce in literature. In the recent work of Sun et al. [3] high-pressure laminar flame speed measurements are reported to validate a chemical reaction mechanism for H_2–CO mixtures using a dual-chamber apparatus that generates an outwardly propagating premixed flame. The experiments were however, reported mostly for rich mixtures with 1% H_2 to 50% H_2 in the fuel mixture. A study of Natarajan et al. [1] uses a conical flame for determining S_L at elevated pressure and temperature for similar fuel mixtures. Burke et al. [4] used the outwardly propagating flame technique to determine mass burning rates for 50% and 10% H_2 in the H_2–CO fuel mixture with an equivalence ratio of 2.5. In the most recent work of Krejci et al. [6] and Kéromnès et al. [7], constant volume cylindrical vessels are used to determine S_L of H_2–CO mixtures. The reported results are mostly for 50% and higher CO concentration in the fuel mixture.

The objectives of the present work were (1) to provide new experimental laminar burning velocity results of lean H_2–CO mixtures (50:50% and 85:15% by volume) obtained with a variety of oxidizers (O_2/N_2/He) using the heat flux method at elevated pressure, (2) to propose an updated kinetic mechanism for H_2–CO combustion based on the mechanism of Konnov [8] and (3) to validate the proposed mechanism with new experimental results and those from the literature which include laminar burning velocity, ignition delay time and speciation data.

2. High-pressure experiments using heat flux method

Experiments were conducted at elevated pressure using the high-pressure heat flux method installation [9] recently extended to pressures greater than atmospheric pressure. The heat flux method makes use of the fact that the heat loss from the flame needed to stabilize it on the burner can be compensated by adding heat to the unburnt gas mixture. A schematic representation of the experimental setup is shown in Fig. 1. A perforated plate is fitted on a burner head (Fig. 2(left)). The burner head is maintained at a temperature higher than the unburnt gas temperature by heating it (85 °C) at the edge at radius 15 mm. This provides a heat transport from the burner head to the burner plate and subsequently to the unburnt gas mixture. The balance in heat flux is reflected in the temperature profile of the burner plate.

The unburnt gas mixture flows through the plenum chamber of the burner which is maintained at 25 °C using a water thermal bath. The burner head is jacketed with a water thermal bath at 85 °C. Eight Copper–Constantan thermocouples are soldered at different radial positions, r, on the perforated burner plate with holes of 0.3 mm diameter and 0.4 mm pitch shown in Fig. 2(right). The plate has a thickness of 1 mm. The burner which is rated for pressures up to 10 bar is placed in a high-pressure cell (HPC) (Fig. 3) made of C45 steel. A chimney is placed on top of the vessel through which burnt gases are guided out. A stainless steel connection pipe followed by a needle valve is connected to the exhaust of the chimney. The pressure in the vessel is controlled by this needle valve. When the unburnt gas velocity is higher than the adiabatic burning velocity (super-adiabatic) the heat gain by the gas is larger than the heat loss from the flame. The situation is opposite in case of a sub-adiabatic flame. The only

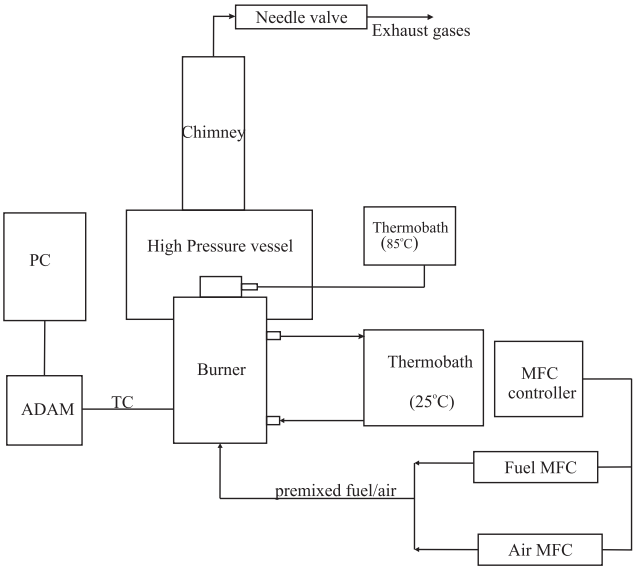

Fig. 1 – Schematic of the high-pressure HFM facility.

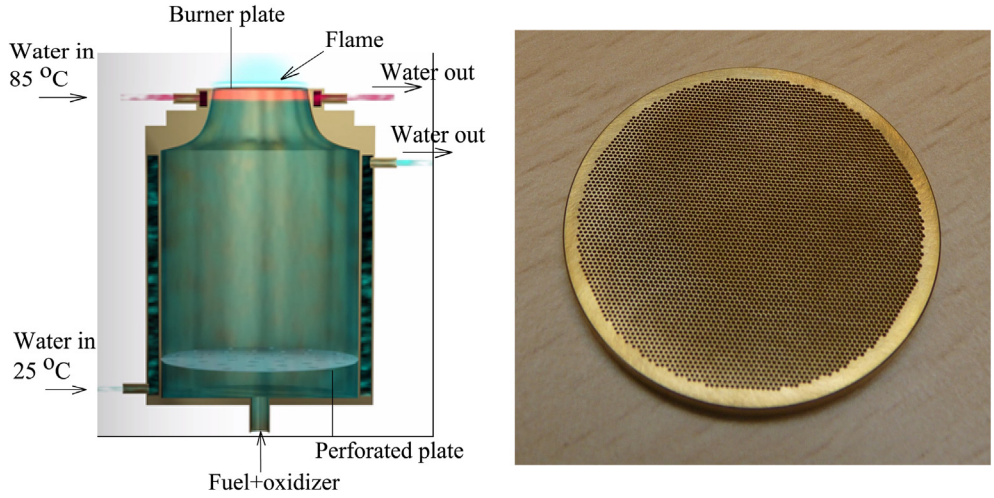

Fig. 2 – (Left) Burner used for heat flux method. (Right) Burner plate (plate diameter = 30 mm, thickness = 1 mm, hole diameter = 0.3 mm, pitch = 0.4 mm).

measurement required in this technique is the temperature profile of the burner plate. The radial profile of temperature on the burner plate close to the adiabatic burning velocity is fitted by the method of least squares to a parabolic profile given by

$$T_p(r) = T_c + \gamma r^2, \quad (1)$$

where $T_p(r)$ is the plate temperature at radius r. T_c is the temperature at the center of the plate, γ is the parabolic coefficient and accounts for the net heat flux between the unburnt gas, plate and the flame. The coefficients of such polynomials are plotted against gas flow velocities. The adiabatic state is reached for zero value of the parabolic coefficient γ. A more detailed description of the concept, principle and error estimation is discussed by Bosschaart and de Goey [5]. Error component from volume flow rate, pressure, temperature of the unburnt gas mixture and scattering in thermocouple measurements amount to the total error in measured S_L. The maximum error in the present work resulting from the scatter in the thermocouples is 1.5 cm/s.

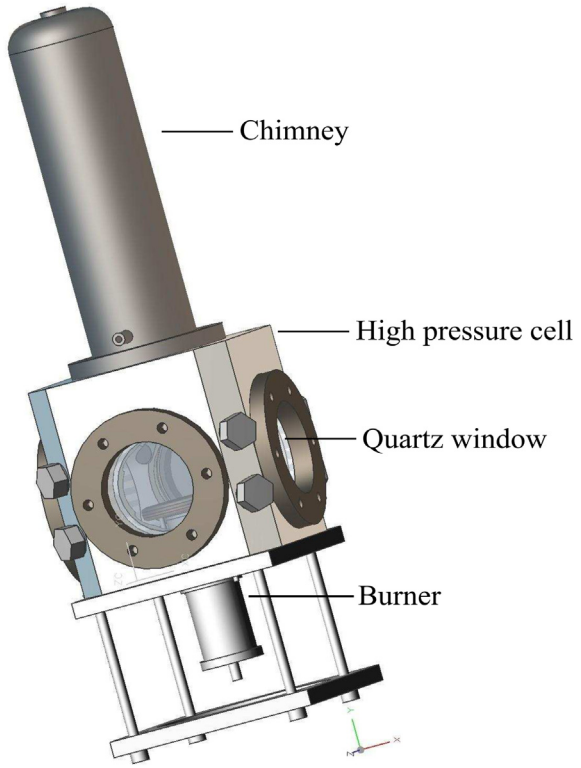

Fig. 3 – High-pressure system rated up to 10 bar.

This method was initially applied to CH_4–air flames up to 5 atm [9]. The results agreed well with reported data available in the literature. To proceed with H_2–CO mixtures, a number of additions had to be made in order to ensure accuracy and safe working environment. Since these mixtures contained CO, special attention was paid towards the safety aspects including a detection system and tested high-pressure lines. In addition, a special N_2-flushing line was introduced to keep the fuel line flushed when not in use. This ensured that no harmful gases could leak into the laboratory. In addition to this, it was also observed that CO when stored in iron or nickel based cylinders or stainless steel flow lines, some of the gas converts into compounds like carbonyls [10]. When the mixture is lighted, the flame emits a pale, off-white color. This indicates that the mixture is not pure anymore. Hence, special care was taken to install brass and copper lines. High purity of the gases was ensured before the experiments. It was also ensured that all the components could withstand pressures as high as at least 10 bar. Mass flow controllers were calibrated before performing experiments.

The tests were focused on 50:50% and 85:15% H_2–CO mixtures. In industrial conditions, these mixtures are burnt with air. This results in very high burning velocity. However, the heat flux method is best operational with a burning velocity not higher than 80 cm/s with the above mentioned dimensions of the plate perforations [11]. With flows higher than 80 cm/s, the flame may not be flat anymore. The outlet length of unburnt gas mixture individual jets increases and

creates curved flames. This effect is likely to increase even at elevated pressure since length scales decrease. The burner plate hole diameter and the distance between the holes play an important role and have been reduced for that matter [11]. Furthermore, the oxidizers are diluted with inert gases to obtain lower burning velocity which suits the burner plate used in the experiments. Table 1 summarizes all the experiments that were performed for the present work.

A flame from the heat flux method is one-dimensional and does not exhibit any kind of instability/disturbance. Initially, the burner head was heated with an electrical heater [9]. With each experiment special attention was paid to ensure proper conduction of heat from the heater to the burner head. In the absence of proper conduction, acoustical instabilities were observed in the flame. Therefore, a new burner design was proposed and implemented in the present experiments where electrical heater was replaced by water bath heater which ensured better heat conduction.

3. Experimental results

H_2–CO mixtures were introduced to the heat flux method system first at atmospheric conditions. Fig. 4(left) shows the variation of laminar burning velocity of 50:50% H_2–CO and air mixture at 1 atm for a wide range of equivalence ratios (0.5–5). Experimental results are from Refs. [3,6,12–14]. Using a close-up view of the lean side of the mixture, results from the present work is shown in Fig. 4(right). The results are well in agreement with the literature data [1,3,6,12].

For pressures larger than 4 atm, the flame with the O_2–N_2 oxidizer shows cellular/structural instabilities due thermo-diffusive and hydrodynamic instabilities (see Fig. 5(left)). Due to the low mixture Lewis number, the flame exhibits such behavior at higher pressure. A similar behavior has been reported by Natarajan et al. [1] and Sun et al. [3]. The picture in Fig. 5(right) shows a stable 50:50% H_2–CO flame at 8.5 atm in a slightly super-adiabatic state.

The experimental results reported in Figs. 6–8 show a decrease in laminar burning velocity with increase in pressure. Fig. 6(left) depicts the results of 50:50% H_2–CO flames for pressures up to 5 atm with diluted oxidizers. With similar concentration of O_2 in both oxidizers and leaner mixtures of O_2–He, large differences are noticed in the laminar burning velocity. Diluent impact on laminar burning velocity has been well described by Galmiche et al. [15]. A lower heat capacity and resulting higher thermal diffusivity of helium than nitrogen results in higher laminar burning velocities. Laminar burning velocity of 50:50% H_2–CO and 15:85% O_2–N_2 for pressure up to 4 atm and $\phi = 0.7$ are shown in Fig. 6(right).

With time these experiments were repeated to gain experience and stability in operation. Since it was observed that the most stable and flat flames were obtained with O_2–He oxidizer, the rest of the measurements were carried out at different proportions of this oxidizer. Moreover, the objective of the experiment was to reach lean conditions so as to validate the proposed kinetic scheme. With an oxidizer mixture of 12.5% O_2 and the rest helium, 50:50% H_2–CO flame were obtained at $\phi = 0.6$ up to a pressure of 9 atm as shown in Fig. 7. The flames were highly sensitive to variations in velocity/heat flux as the pressure was increased. Change in gas velocity by 1–1.5 cm/s from the adiabatic state showed non-flat structures (super-adiabatic) or moved closer to the burner plate thereby increasing the plate temperature (sub-adiabatic) considerably.

Fig. 8 shows laminar burning velocity results of 85:15% H_2–CO flames. During the experiments of such H_2-rich fuel mixtures an equivalence ratio of 0.5 was achieved with 12% O_2 in the O_2–He oxidizer mixture up to a pressure of 8 atm that corresponds to an adiabatic flame temperature of 1470 K.

The continuous black line in the above comparisons (Figs. 4, 6–8) represents the proposed model prediction from the present study. Recent models from literature are also presented for comparison [7,17]. Model prediction using the proposed kinetic scheme in the present work agrees well with the experimentally determined results. Models from Li et al. [17] and Kéromnès et al. [7], in general, over-predict the measured results, more evidently for 85:15% H_2–CO mixtures. For the same mixture at $\phi = 0.5$ (Fig. 8(right)), the models from the literature over-predict S_L by 20 cm/s. Our model shows much better agreement even though a difference of ~6 cm/s still exists. This difference can be attributed to the uncertainties in the kinetic model. The subsequent sections discuss the proposed kinetic model and comparisons with experimental data from literature.

Table 1 – Measurement conditions.

Fuel	H_2/CO (50:50%)	H_2/CO (85:15%)
Oxidizer	Air	
	O_2/N_2 (15:85%)	O_2/N_2 (15:85%)
	O_2/N_2 (10:90%)	O_2/He (12:88%)
	O_2/He (10:90%)	
	O_2/He (12.5:87.5%)	
ϕ	0.6–1.0	0.5–0.7
T (°C)	25	25
P (atm)	1–9	1–8

4. Kinetic modeling

The in-house laminar code CHEM1D [18] was used for modeling a one-dimensional free flame for the determination of the flame temperatures and laminar burning velocity. CHEM1D solves a set of equations describing the conservation of mass, momentum, energy and chemical components for chemically reacting flows. It uses an exponential finite-volume discretization in space and non-linear differential equations are solved with a fully implicit, modified Newton method along with a complex transport model. An adaptive gridding procedure is also implemented to increase accuracy in the flame front by placing almost 80% of the grid points in the area with the largest gradients. Thermodynamic data used are all from the database of Burcat and Ruscic [19].

Many studies have been conducted in the past to analyze the hydrogen flame structure and kinetic pathways. Reaction numbering corresponds to the list given in Table 2 which outlines the chemical scheme proposed in the present work. It is known that CO–O_2 mixtures without hydrogen-containing

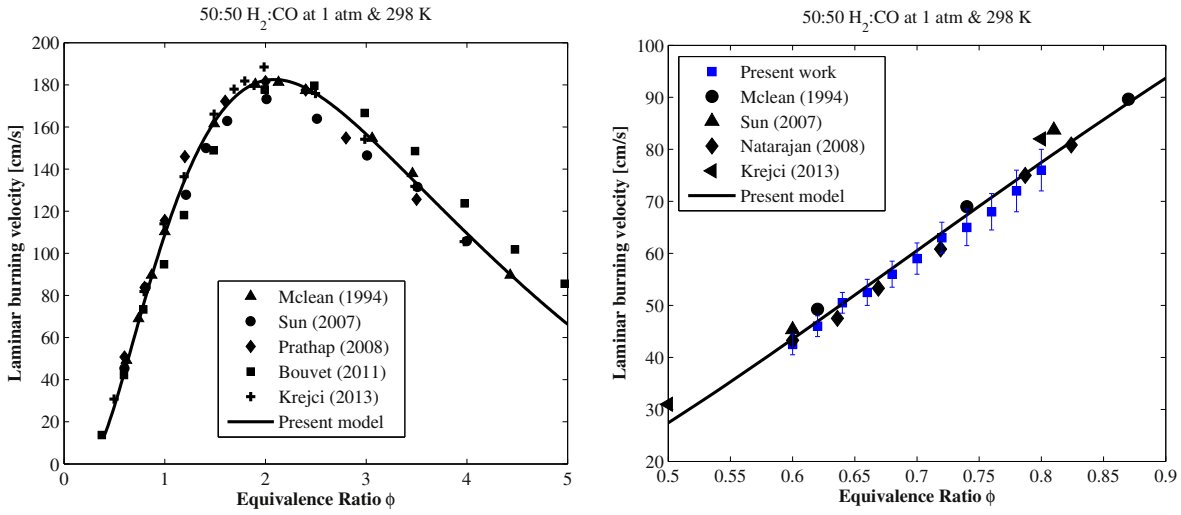

Fig. 4 – Laminar burning velocity of 50:50% H_2–CO/Air mixture at atmospheric pressure and 298 K. Symbols: (Left) Experiments from literature [3,6,12–14]. (Right) Comparison of present experiments with literature [1,3,6,12]. Line: Simulation using present model.

additives react very slowly since oxidation includes only two steps CO + O_2 = CO_2 + O (25) and CO + O (+M) = CO_2 (+M) (22). In the presence of traces of hydrogen, water or hydrocarbons, the chain process develops fast with participation of H, OH, and HO_2 radicals and the CO oxidation proceeds mainly through reactions CO + OH = CO_2 + H (23) and CO + HO_2 = CO_2 + OH (26). With 50% CO or less in the fuel mixture, the process is dominated by hydrogen chemistry. In such a case, the consumption of H, OH and HO_2 shows a large influence especially at elevated pressure [4]. The original Konnov mechanism [8] is tested at elevated pressures in a few studies and reported insufficient [4,20]. The mechanism is updated in the present work with some modifications, taking into account recent evaluated kinetic data for combustion modeling. The CO reaction set is included from Konnov 0.6 version [21] for hydrocarbons with few modifications which are discussed later in this section. Reaction flux, species flux and sensitivity analysis of lean H_2–CO mixtures were performed using the proposed kinetic model at elevated pressure to identify important reactions.

Fig. 9 represents the rate of important reactions in H_2–CO chemistry in the lean regime through a combustion process at different pressures and H_2 addition. The plots come in assistance in representing the competing pathways for high-pressure kinetics of the chain branching reaction H + O_2 = OH + O (8) and the pressure-dependent reaction H + O_2 (+M) = HO_2 (+M) (5a) at ϕ = 0.5 and adiabatic flame temperature of 1500 K at pressure 1, 5 and 10 atm for different H_2–CO mixtures. Reaction (8) moves ahead of (5) with an increase in H_2 concentration in the fuel mixture at atmospheric pressure, however, not considerably. With an increase in pressure, HO_2 production is found important in all cases. The fuel mixture without CO concentration sees the highest HO_2 production due to higher availability of H_2O as the third body.

HO_2 radical fraction changes steep gradients as suggested by Fig. 10 with pressure (1, 5 and 10 atm at ϕ = 0.5 and adiabatic flame temperature, T_f of 1500 K). The rate constants of both reactions (5) and (8) need proper treatment as is suggested in various literature sources. Among other competing pathways H + HO_2 set, reaction (12) (H + HO_2 = OH + OH)

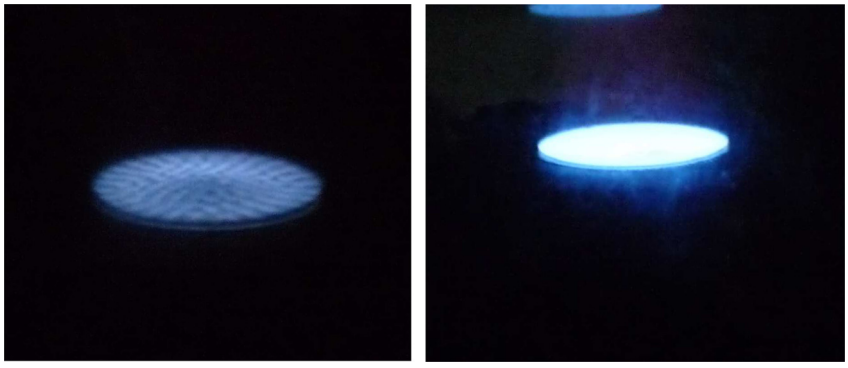

Fig. 5 – (Left) Structural instability in 50:50% H_2–CO flame with O_2–N_2 at 5 atm. (Right) 50:50% H_2–CO flame with O_2–He at 8.5 atm and ϕ = 0.6.

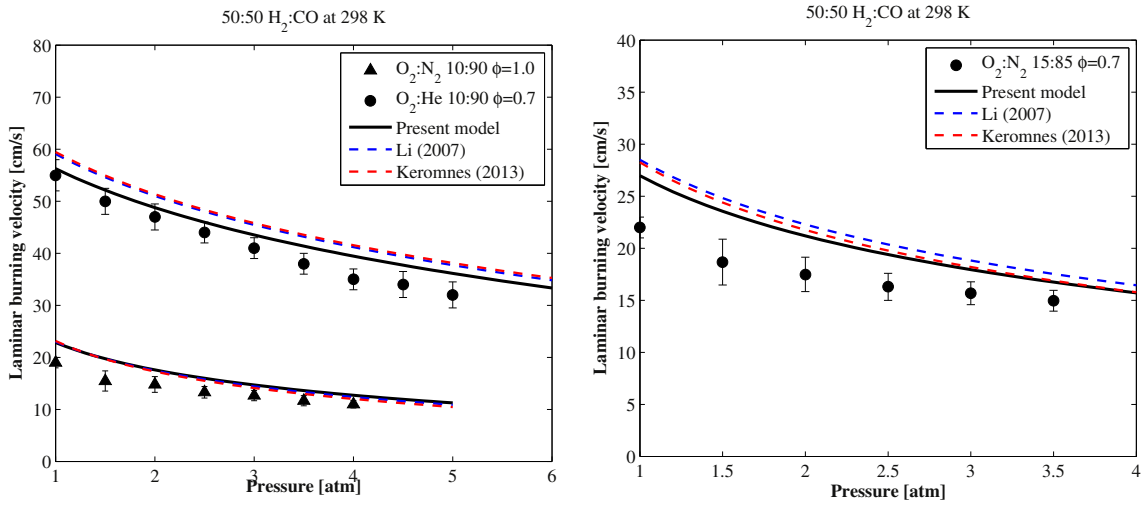

Fig. 6 – (Left) Laminar burning velocity of 50:50% H_2–CO mixture. Symbols: Experiments – Triangles: with O_2–N_2 (10% O_2) at $\phi = 1.0$ and Circles: O_2–He (10% O_2) at $\phi = 0.7$. (Right) Laminar burning velocity of 50:50% H_2–CO mixture with O_2–N_2 (15% O_2) at $\phi = 0.7$. Symbols: Experiments. Line: Simulation – present model (black), Li et al. [17] (blue) and Kéromnès et al. [7] (red). (For interpretation of the references to color in this figure legend, the reader is referred to the web version of this article.)

shows very high contribution in OH production which in turn assists reaction (8). Higher sensitivity of reaction (8) can be attributed to this reason. It has been reported in earlier studies that reaction (8) in all cases remains the most sensitive reaction. The reaction (13), ($H + HO_2 = H_2 + O_2$) contributes uniformly in all cases when compared to other reactions. Sensitivity of reaction (36), namely $CO + OH = CO_2 + H$ remains high with a gradual decrease in H_2-rich fuel mixtures.

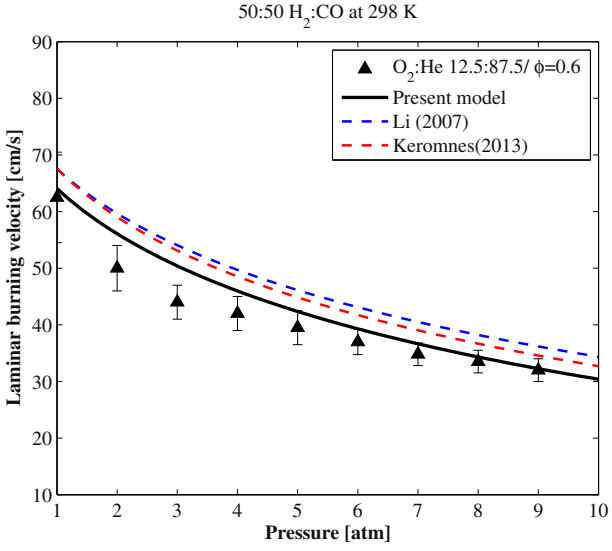

Fig. 7 – Laminar burning velocity of 50:50% H_2–CO mixture with O_2–He (12.5% O_2) at $\phi = 0.6$. Symbols: Experiments. Lines: Simulations – present model (black), Li et al. [17] (blue) and Kéromnès et al. [7] (red). (For interpretation of the references to color in this figure legend, the reader is referred to the web version of this article.)

In general, it is apparent from sensitivity analysis that all reactions involving H, OH and HO_2 contribute significantly to the performance of the mechanism and the combustion process. The kinetic behavior of mixtures containing a CO mole fraction more than 50% in the fuel mixture is expected to affect the oxidation of both H_2 and CO. HCO production from various pathways (through H and OH) contributes towards CO oxidation. Higher OH concentration reacts with both CO and H_2 and oxidizes to stable species. However, at elevated pressure, HO_2 gets consumed to obtain HCO which in turn oxidizes directly or eventually to CO_2. With lower concentration of CO, this pathway becomes less important.

The rest of this section outlines the rate constants modified to the original mechanism. In proposing the updated scheme no attempt is made in adjusting the rate constants to fit the experimental data. Adjustment of rate constants to fit experimental data distorts the original fit/derivation proposed for the individual reactions.

The rate constant of reaction (7), $O + H_2 = OH + H$ has been reviewed a number of times and has been of great experimental interest. Due to its variation at high and low temperature and also its high significance in hydrogen chemistry, the rate constant finds significant importance in the hydrogen mechanism. This reaction is one of the pathways to the formation of OH that in turn gives a path to NO formation through thermal NO_x mechanism. In the work of Baulch et al. [22], a review has been performed ever since 1972 including Cohen and Westberg [23] and Tsang and Hampson [24]. The mechanism of Konnov [8] adopted the rate constant derived by Sutherland et al. [25] which extrapolates even to high temperatures (1700–3500 K). In the present mechanism a slightly improved value of Baulch et al. [22] is adopted that also fits low temperature data.

The reaction $H + O_2 = OH + O$ (8) signifies chain branching and the production of OH radicals which are of importance to hydrogen combustion and NO_x chemistry.

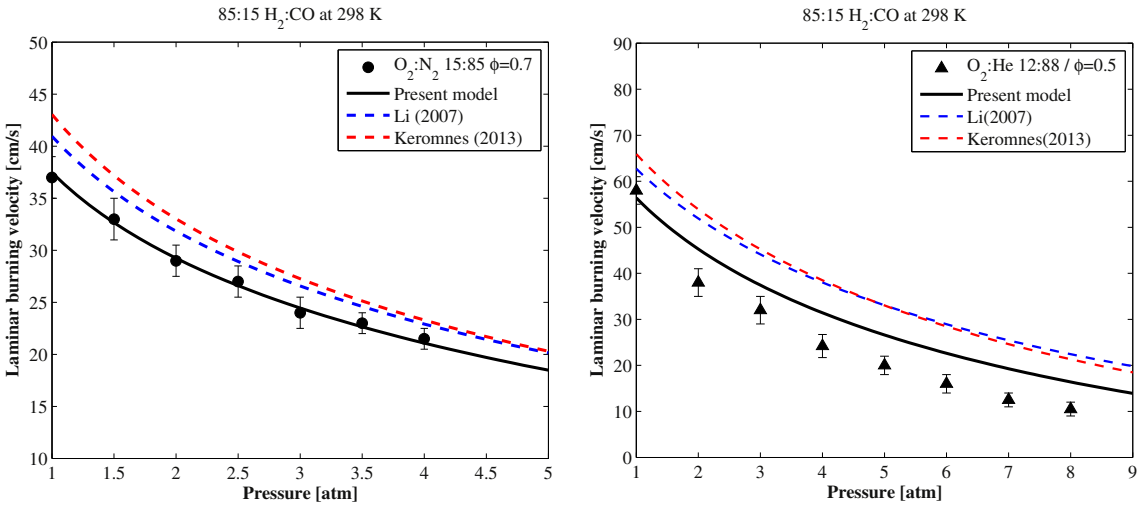

Fig. 8 – (Left) Laminar burning velocity of 85:15% H_2–CO mixture with O_2–N_2 (15% O_2) at $\phi = 0.7$. (Right) Laminar burning velocity of 85:15% H_2–CO mixture with O_2–He (12% O_2) at $\phi = 0.5$. Symbols: Experiments. Lines: Simulations – present model (black), Li et al. [17] (blue) and Kéromnès et al. [7] (red). (For interpretation of the references to color in this figure legend, the reader is referred to the web version of this article.)

Various experiments have been performed to determine the rate constant of this reaction but only at temperatures greater than 500 K. Low temperature experiments have not been possible resulting in prohibition of consistent results over a sufficiently wide temperature range. Baulch et al. [22] reviewed data from a number of sources, mostly shock tube experiments, for pressure up to 4 bar. In the review, from the experimental and simulation results of Hwang et al. [26] the rate constant finds a non-Arrhenius expression defined for a temperature range of 950–3100 K. A recent study of Hong et al. [27] proposes an Arrhenius fit which has been applied in the present model.

For lower temperatures a number of studies are available in the literature and hence evaluations of rate constants for reactions $H + HO_2 = OH + OH$ (12) and $H + HO_2 = H_2 + O_2$ (13) have been accepted. However, at higher temperatures the data are scarce. Mueller et al. [28] performed flow reactor studies and determined the rate constants of the above reactions for a range of temperatures and pressures. They inferred with a compilation of data depicting the kinetic response of the $H_2/O_2/N_2$ mixture to changes of pressure (up to 100 atm) and stoichiometry with new explosion limit data. As per their conclusions the reaction $H + HO_2 = H_2 + O_2$ shows a high sensitivity towards lean conditions and is more important than the other competing reactions. The rate constants recommended by Mueller et al. [28] have been included in the present mechanism. The third possible route $HO_2 + H = H_2O + O$ has not been included in many previous studies due to its large uncertainty in the rate constant due to the slow nature of the reaction. The recommendation of Baulch et al. [22] is included in the present study.

The peculiarities of the rate constant of reaction, $CO + O (+M) = CO_2 (+M)$ (22) were analyzed in a number of studies [29–32]. Allen et al. [33] proposed to combine the low-pressure rate constant expression from Westmoreland et al. [32] fit to a modified Arrhenius form and Troe's [29] high-pressure rate constant using a Lindemann fit [30]. Warnatz et al. [34] modified the recommended low-pressure rate constant of Warnatz [31] within 1000–3000 K multiplying it by a factor of 1.34. Davis et al. [35] evaluated the uncertainty factor of this rate as 2, and in the optimization procedure proposed to multiply the rate constant of Allen et al. [33] by a factor of 0.76. In the present work the expression of Allen et al. [33] was adopted with the uncertainty factor of 2.

Temperature and pressure dependence of the rate constant of reaction, $CO + OH = CO_2 + H$ (23) was a subject of many experimental and theoretical studies. Experimental studies and reviews prior to 2004 were summarized by Baulch et al. [22]. Rate constants derived by Troe [36] were largely based on the experiments of Fulle et al. [37]. They have been accepted as recommendations by Baulch et al. [22]. The involvement of formation of the intermediate species HOCO and hence pressure and temperature dependence is argued by Troe [36]. Li et al. [17] also acknowledge this fact and determined a rate constant by fitting experimentally measured rate constants available in literature by the method of least squares. Regrettably most of the recent studies are theory. The expression of Li et al. [17] has been adopted in this study.

The rate constant of the pressure-dependent reaction $CO + OH (+M) = HOCO (+M)$ (24) was derived based on Troe [29] and proceeds mainly at low temperatures [17]. CO concentration is also influenced by reaction, $CO + HO_2 = CO_2 + OH$ (26). Kim et al. [38] and Tsang and Hampson [24] suggested rate constants that were reported by Sivaramakrishnan et al. [39] to have much higher uncertainty. This reaction becomes important during the chemical induction period as it has significant heat release at that stage. Through experimental studies Mittal et al. [40] suggested the use of a revised lower value than Baulch et al. [22], especially for temperatures around 1000 K. Sun et al. [3] performed calculations based on ab initio theory and canonical transition state theory to

Table 2 – Reactions and rate constants of the proposed H_2–CO kinetic mechanism, $k = AT^n \exp(-E_a/RT)$. Units are cm^3 mol s cal K.

No.	Reaction	A	n	E_a	Reference
1a	$H + H + M = H_2 + M$ H_2/0.0/N_2/0.0/H/0.0/H_2O/14.3/ CO/3.0/CO_2/3.0/	7.000E+17	−1.0	0.0	[23]
1b	$H + H + H_2 = H_2 + H_2$	1.000E+17	−0.6	0.0	[23]
1c	$H + H + N_2 = H_2 + N_2$	5.400E+18	−1.3	0.0	[23]
1d	$H + H + H = H_2 + H$	3.200E+15	0.0	0.0	[23]
2	$O + O + M = O_2 + M$ O/28.8/O_2/8.0/N_2/2.0/H_2O/5.0/	1.000E+17	−1.0	0.0	[31]
3	$O + H + M = OH + M$ H_2O/5.0/	6.750E+18	−1.0	0.0	[60]
4a	$H_2O + M = H + OH + M$ H_2O/0/H_2/3/N_2/2/O_2/1.5/CO_2/4/	6.06E+27	−3.312	120,770	[1]
4b	$H_2O + H_2O = H + OH + H_2O$	1.E+26	−2.44	120,160	[1]
5a	$H + O_2(+M) = HO_2(+M)$ LOW/5.70E+19 −1.4 0.0/ TROE/0.5 100000 10/ H_2O/0.0/O_2/0.0/H_2/1.5/CO_2/ 2.4/He/1.0/Ar/0.0/	4.660E+12	0.44	0.0	[61]
5b	$H + O_2(+Ar) = HO_2(+Ar)$ LOW/7.430E+18 −1.2 0.0/ TROE/0.5 10 100000/	4.660E+12	0.44	0.0	[61]
5c	$H + O_2(+O_2) = HO_2(+O_2)$ LOW/5.690E+18 −1.094 0.0/ TROE/0.5 100000 10/	4.660E+12	0.44	0.0	[61]
5d	$H + O_2(+H_2O) = HO_2(+H_2O)$ LOW/3.670E+19 −1.0 0.0/ TROE/0.8 10 100000/	9.060E+12	0.2	0.0	[62]
6a	$OH + OH(+M) = H_2O_2(+M)$ LOW/2.38E+19 −0.8 0.0/ TROE/0.5 100000 10/ H_2O/0.0/	1E+14	−0.37	0.0	[8,22]
6b	$OH + OH(+H_2O) = H_2O_2(+H_2O)$ LOW/1.45E+18 0.0 0.0/ TROE/0.5 100000 10/	1E+14	−0.37	0.0	[8,22]
7	$O + H_2 = OH + H$	3.82E+12 +8.79E+14	0.0 0.0	7948 19,170	[22]
8	$H + O_2 = OH + O$	1.04E+14	0.0	15286	[27]
9	$H_2 + OH = H_2O + H$	2.140E+08	1.52	3450	[22]
10	$OH + OH = H_2O + O$	3.34E+04	2.42	−1930	[22]
11	$HO_2 + O = OH + O_2$	1.630E+13	0.0	−445	[63]
12	$H + HO_2 = OH + OH$	7.08E+13	0.0	295	[28]
13	$H + HO_2 = H_2 + O_2$	1.66E+13	0.0	823	[28]
14	$H + HO_2 = H_2O + O$	1.45E+12	0.0	0.0	[22]
15	$H_2 + O_2 = OH + OH$	2.040E+12	0.44	69,155	[64]
16	$HO_2 + OH = H_2O + O_2$	2.89E13 +9.270E+15	0.0 0.0	−500 17,500	[22]
17a	$HO_2 + HO_2 = H_2O_2 + O_2$	1.030E+14 +1.940E+11	0.0 0.0	11,040 −1409	[65]
17b	$HO_2 + HO_2(+M) = H_2O_2 + O_2 + M$	6.84E+14	0.0	−1950	[66]
18	$H_2O_2 + H = HO_2 + H_2$	1.700E+12	0.0	3755	[22]
19	$H_2O_2 + H = H_2O + OH$	1.000E+13	0.0	3575	[22]
20	$H_2O_2 + O = HO_2 + OH$	9.55E+6	2.0	3970	[24]
21	$H_2O_2 + OH = HO_2 + H_2O$	2.000E+12 +1.700E+18	0.0 0.0	427 29400	[67]
22	$CO + O(+M) = CO_2(+M)$ LOW/1.55E+24 −2.79 4190/ H_2/2.5/H_2O/12/CO/1.9/CO_2/3.8/Ar/0.87/	1.80E+10	0.0	2384	[33]
23	$CO + OH = CO_2 + H$	2.23E+05	1.90	−1160	[17]
24	$CO + OH(+M) = HOCO(+M)$ LOW/7.20E+25 −3.85 1550.0/ TROE/0.6 10.0 100000.0/ H_2/2.5/H_2O/12/CO/1.9/CO_2/3.8/Ar/0.87/	1.20E+07	1.83	−236	[29]
25	$CO + O_2 = CO_2 + O$	2.50E+12	0.0	47,800	[31]
26	$CO + HO_2 = CO_2 + OH$	1.15E+05	2.278	17,545	[3]

Table 2 – (continued)

No.	Reaction	A	n	E_a	Reference
27	HCO + M = H + CO + M H_2/2.5/H_2O/6.2/CO/1.875/CO_2/3.75/Ar/1.0/	4.80E+13	0.0	15,760	[43]
28	HCO + H = CO + H_2	9.00E+13	0.0	0.0	[22]
29	HCO + O = CO + OH	3.00E+13	0.0	0.0	[22]
30	HCO + O = CO_2 + H	3.00E+13	0.0	0.0	[22]
31	HCO + OH = CO + H_2O	1.00E+14	0.0	0.0	[22]
32	HCO + O_2 = CO + HO_2	2.71E+10	0.68	−471	[22]
33	HCO + HO_2 = CO_2 + OH + H	3.00E+13	0.0	0.0	[24]
34	HCO + HO_2 = CO + H_2O_2	3.00E+12	0.0	0.0	[24]
35	HCO + HCO = CH_2O + CO	2.70E+13	0.0	0.0	[44]
36	HCO + HCO = H_2+CO + CO	3.00E+12	0.0	0.0	[24]
37	HOCO(+M) = H + CO_2(+M) LOW/2.29E+26 −3.02 35070/ H_2/1.5/H_2O/0.0/O2/0.0/Ar/0/	1.74E+12	0.307	32,930	[45]
38	HOCO + OH = H_2O + CO_2	1.60E+13	0.0	560	[46]
39	HOCO + O_2 = HO_2+CO_2	1.38E+10	0.842	160	[51]

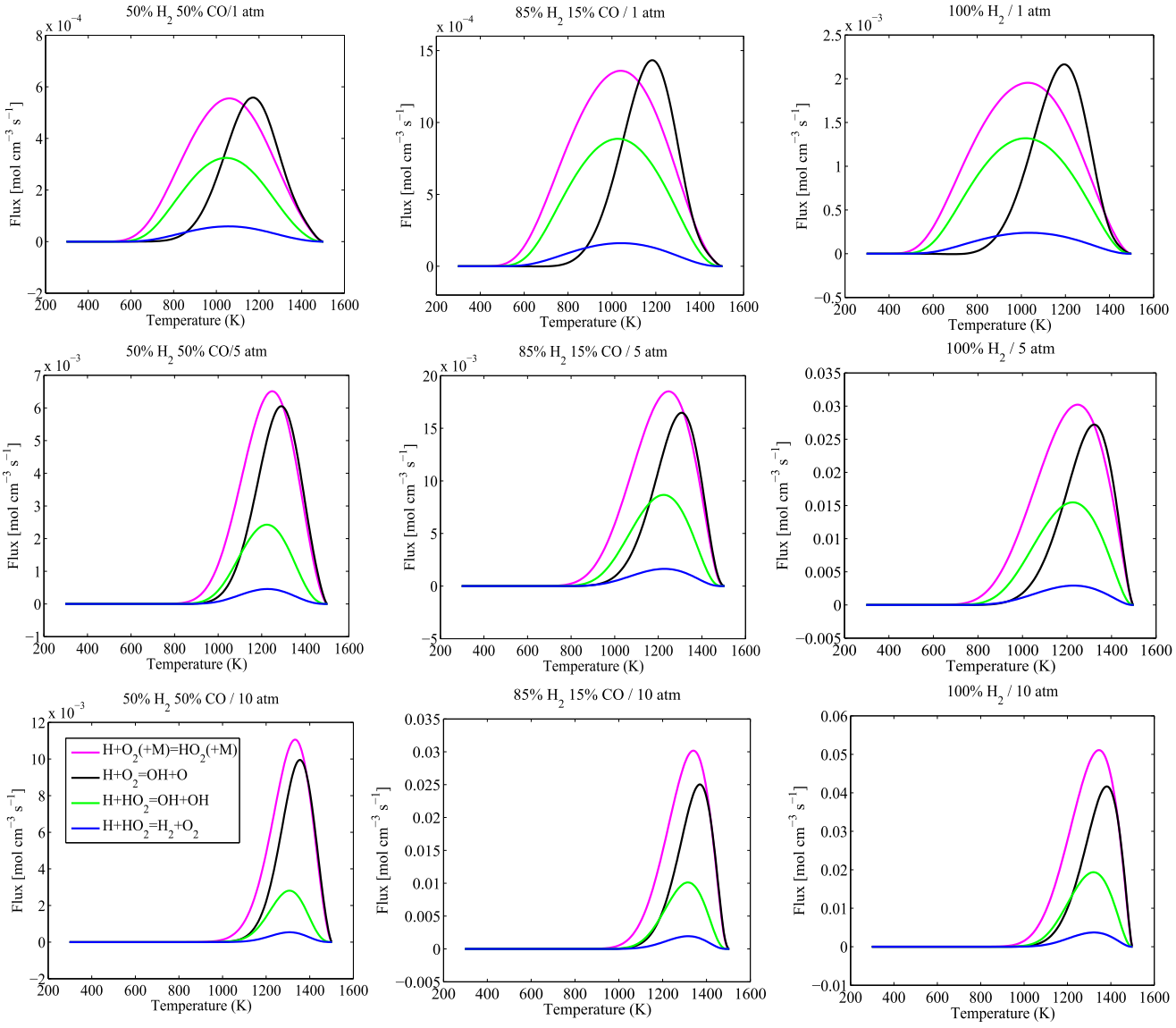

Fig. 9 – Comparison of rate of reactions for H_2/CO/O_2/He flames at P = 1, 5, 10 atm, ϕ = 0.5 and T_f ~ 1500 K.

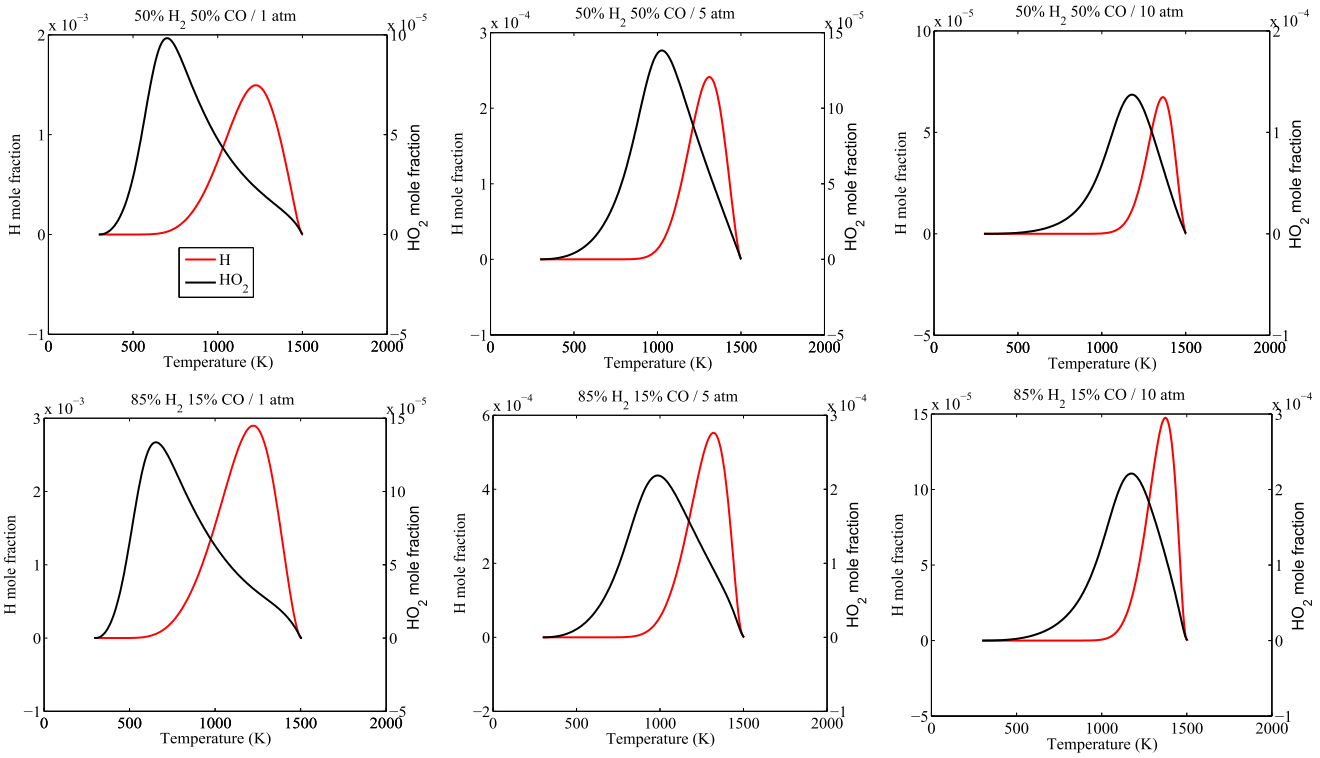

Fig. 10 – Comparison of H and HO_2 mole fraction for $H_2/CO/O_2$/He flames $P = 1, 5, 10$ atm, $\phi = 0.5$ and $T_f \sim 1500$ K.

determine the reaction rate constant which has been used in the present study.

Decomposition of formyl radical in HCO + M = H + CO + M (27) is the main pathway to generate CO at high temperature. Timonen et al. [41] studied the reaction of HCO with four molecules as a function of temperature in a tubular reactor and determined their rate constants. Study by Li et al. [17] inferred that the rate is two times lower than that of Timonen et al. [41]. Zhao et al. [42] showed that the reaction is most sensitive to certain temperature range. Li et al. [17] recommended a weighted least square fitting to all experimental data available in the literature and yielded a new correlation. Baulch et al. [43] reviewed the rate constants prior to 1992 and recommended a value which is being used in the present study.

Reaction (32), HCO + O_2 = CO + HO_2 has a rate constant based on the reviews and evaluations of Baulch et al. [22]. Reaction between hydroperoxy radical and formyl radical HCO + HO_2 = CO + H_2O_2 (34) has not been studied experimentally. Tsang and Hampson [24] estimated the total rate constant with a high uncertainty of a factor of 5 and this value

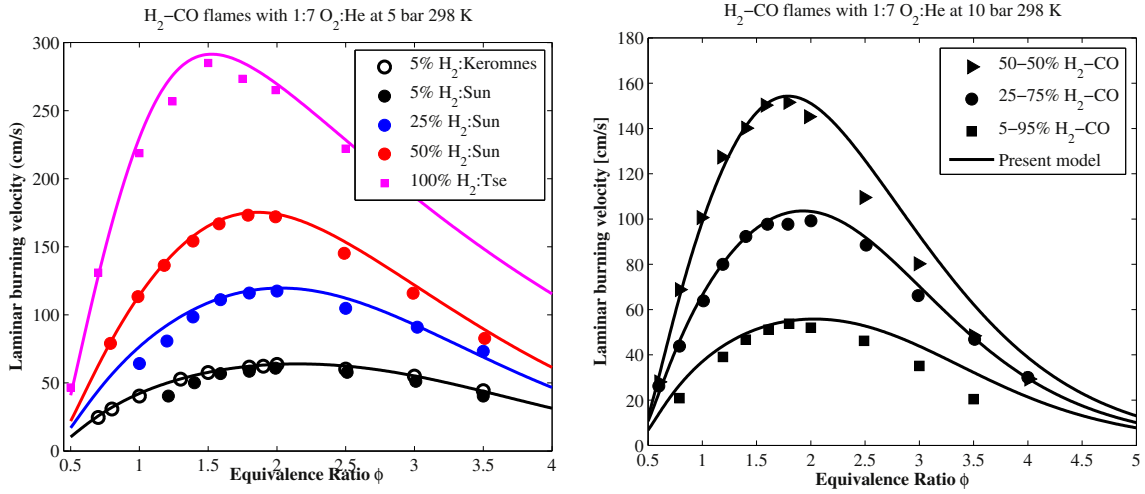

Fig. 11 – H_2–CO flame (Left) 5 atm. Symbols: Experiments [3,7,52] (Right) 10 atm. Symbols: Experiments [3]. Lines: Present model.

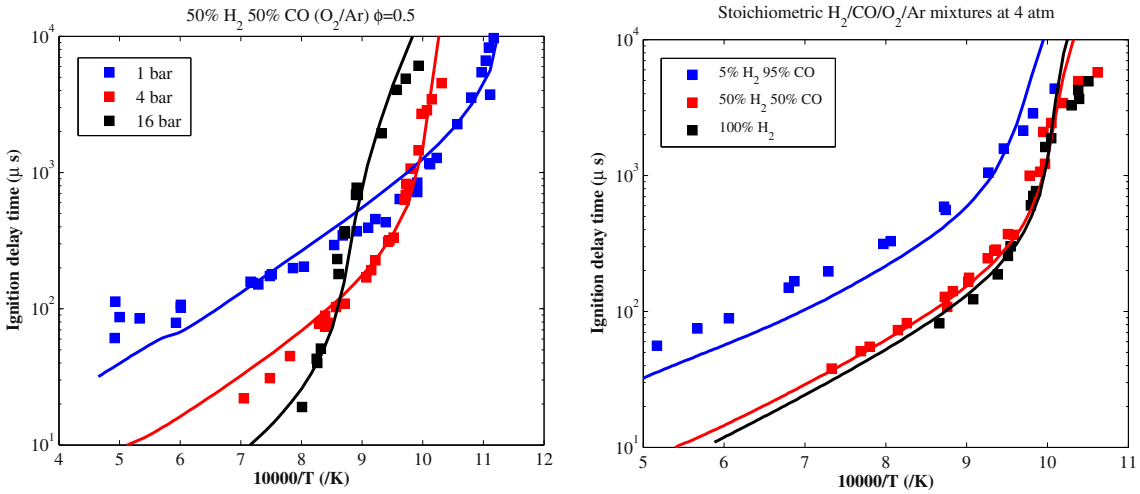

Fig. 12 – (Left) 50% H_2 50% CO O_2/Ar mixture, $\phi = 0.5$. (Right) Different H_2/CO/O_2/Ar mixtures at $\phi = 1.0$ and 4 atm; Symbols: Experiments [7]. Lines: Present model.

is included in the present model. The second channel (34) was assumed minor with a rate 10 times smaller.

Self-reaction between HCO radicals includes two channels HCO + HCO = CH_2O + CO (35) and HCO + HCO = CO + CO + H_2 (36). In the majority of kinetic studies reviewed by Baulch et al. [22] these channels were indistinguishable and an overall rate constant within 230–1000 K was given with an uncertainty factor of 1.6 at 300 K rising to 2 at 1000 K. Friedrichs et al. [44] assumed reaction (35) as the major channel and demonstrated that at temperatures below 820 K concentration time profiles of HCO are affected by this reaction. Therefore, it should be considered in kinetic models developed for these intermediate temperatures. In the present study the temperature-independent rate constant of Friedrichs et al. [44] was attributed to reaction (35).

Reaction HOCO (+M) = H + CO_2 (+M) (37) derives its rate constant from Larson et al. [45]. This reaction proceeds as an intermediate to the reaction (24). The reaction is temperature dependent over a narrow range of 200–360 K. The rate constant of reaction HOCO + OH = H_2O + CO_2 (38) has never been measured. Yu et al. [46] performed ab initio dynamic calculations of the thermal rate constant from 250 to 800 K. Due to some uncertainty of the calculations at temperatures around 400 K, the rate constant was approximated in the present work by a simple Arrhenius expression listed in Table 2 with an estimated uncertainty factor of 2. The rate constant of reaction HOCO + O_2 = HO_2 + CO_2 (39) was measured only at room temperature [47–49]. Poggi and Francisco [50] performed ab initio calculations and found calculated barrier of an adduct formation with eventual dissociation into products of 1.6 kcal/mol. Yu and Muckerman [51] extended these calculations using a direct dynamic method and calculated thermal rate constant from 200 to 1000 K. The value obtained at room temperature was in good agreement with available measurements. In the present work the results of Yu and Muckerman [51] were approximated by the non-Arrhenius expression shown in Table 2. The uncertainty factors of this reaction were evaluated as 2 taking into account experimental scattering and the uncertainty of the modeling of Yu and Muckerman [51].

5. Model validation using literature data

After validating the proposed kinetic mechanism with new measurements as shown in earlier section, the scheme was further validated using experimental data available in the recent literature. In general, the scheme is observed to be performing well against all the cited experiments.

5.1. *Laminar burning velocity*

Experimental results of lean H_2–CO mixtures at elevated pressure are scarce in literature. In view of the applicability of the proposed model, the validations were carried out with CHEM1D at all conditions. Fig. 11(left) shows the variation of the laminar burning velocity of H_2–CO mixtures with respect to equivalence ratio at 5 atm and 298 K. The proposed model agrees well with the experimental data of Kéromnès et al. [7], Sun et al. [3] and Tse et al. [52]. Fig. 11(right) depicts various H_2–CO flames at 10 atm from Sun et al. [3]. The model predicts well especially in the lean region.

5.2. *Ignition delay time*

Shock tube simulations were performed using a code written by Kazakov [53] as constant pressure adiabatic processes. Fig. 12 shows the variation of ignition delay time with inverse temperature for different H_2/CO/O_2/Ar mixtures at 1, 4 and 16 atm obtained by Kéromnès et al. [7]. The ignition delay time defined in the measurements is the time difference between the initiation of the system by the reflected shock wave and the occurrence of the OH^* maximum. In the modeling, the exact criteria cannot be reproduced because excited species are not included in the mechanism. Ignition delay is defined in the simulations when the pressure gradient reaches the maximum value. Kéromnès et al. [7] also highlighted the fact that the OH^* peak is very close to pressure peak for H_2–CO mixtures for

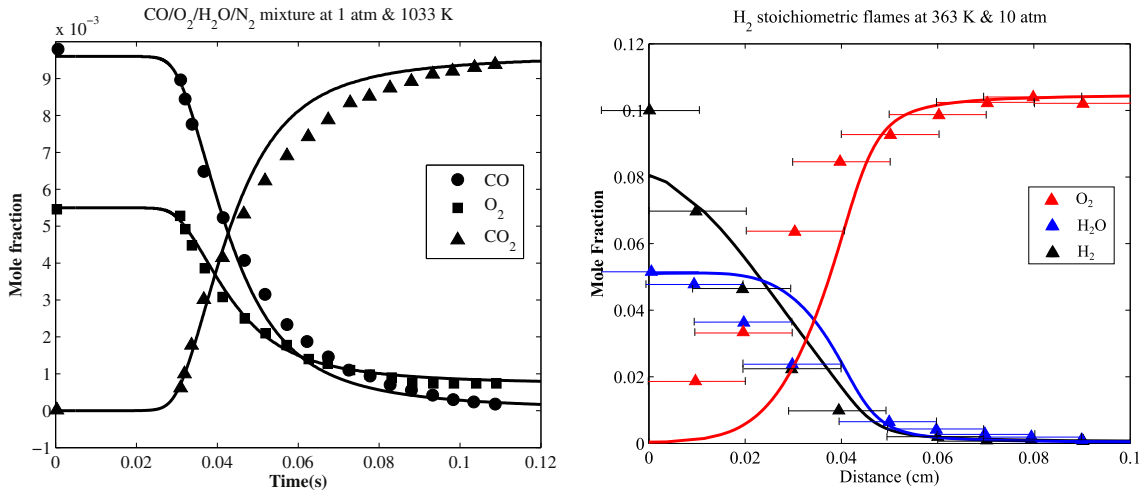

Fig. 13 – (Left) Flow reactor experiment of $CO_2/O_2/H_2O/N_2$ mixture at 1 atm and 1033 K. Symbols: Experiment [57]. Lines: Present model; (Right) Burner stabilized H_2/O_2/Ar flame at 10 atm and 363 K. Symbols: Experiment [58]. Lines: Present model (Black – H_2; red – O_2; blue – H_2O). (For interpretation of the references to color in this figure legend, the reader is referred to the web version of this article.)

CO concentration less than 50%. With higher amounts of CO, a broad OH^* signal is obtained. For this reason, the ignition delay time in Fig. 12(right) is underpredicted in highly (CO) diluted mixture. In general, the present model agrees well with the experimental data. It is also noticed that ignition delay time does not depend on CO dilution for 50:50% H_2–CO and lower. This is because of the rapid oxidation of CO.

5.3. *Species profiles*

Flow reactor measurements are simulated using constant pressure adiabatic processes in SENKIN code [54]. The time axis was shifted as practiced commonly [8,28,55,56] in order to match the calculated data at a reference point of 50% consumption of the major reactant. Fig. 13(left) depicts experimental CO, O_2 and CO_2 profiles in flow reactor with CO(0.96)/O_2(0.55)/H_2O(0.56)/N_2(97.93) mixture at 1 atm and 1033 K from Yetter et al. [57]. The proposed kinetic model follows the species profiles closely.

The present validation was also extended to species profiles of burner stabilized flames. The structure of a stoichiometric H_2 (10%) – O_2 (5%) – Ar (85%) burner stabilized flame was experimentally studied by Paletskii et al. [58] at 1 and 10 atm and initial temperature 363 K using molecular beam inlet mass-spectrometric probing. The study was performed with a spatial resolution of 0.1 mm. At 10 atm, the flame added a further complication of smaller chemical reaction zone (0.7 mm). The agreement between the computed concentration profiles using the present model at 10 atm with the experimental results is satisfactory as shown in Fig. 13(right). A possible reason for this deviation can be that the concentrations measured using the probe that have limited spatial resolution (0.1 mm) are spatially averaged values. This uncertainty is shown by the spatial error bars in the plot. Also, from a previous assessment [59], it was established that the effect of probe intrusion on burner stabilized flames generate uncertainties up to ±200 K for measured temperature profiles which might lead to deviations as shown in Fig. 13(right) especially for H_2 and O_2 species profiles.

6. Conclusions

Stretchless adiabatic laminar burning velocities are determined for lean 50:50% and 85:15% (by volume) H_2–CO mixtures in combination with a variety of oxidizer compositions (O_2/N_2/He) using the heat flux method. The one-dimensional flames are stabilized in a high-pressure environment with zero net heat loss which was reflected in the temperature profile of the burner plate. Experiments at atmospheric pressure agreed well with recent results from literature. Experimental results were obtained for pressures up to 9 atm, for a range of equivalence ratio from 0.5 to 1 at 298 K. An updated H_2–CO kinetic scheme is proposed that includes recently evaluated rate constants from literature. Model validation is performed using results from present experiments and from literature at atmospheric and elevated pressure. At conditions of high pressure and lean combustion, reactions $H + O_2 = OH + O$ and $H + O_2 (+M) = H_2 (+M)$ compete the most when compared to others. Reaction $H + HO_2 = OH + OH$ contributes to OH production, however, less at high-pressure conditions. At higher CO concentrations and leaner mixtures important role of reaction $CO + OH = CO_2 + H$ is observed in subsequent oxidation of CO. It is demonstrated that the proposed model agrees well with the experimental results obtained in the present study and results from literature for lean as well as rich mixtures at elevated pressures.

Acknowledgment

Financial support of this work by the European Union within the 'H_2-IGCC' Project (Grant Agreement No.: 239349) is gratefully acknowledged.

Appendix A. Supplementary material

Supplementary material related to this article can be found at http://dx.doi.org/10.1016/j.ijhydene.2013.10.164.

REFERENCES

[1] Natarajan J, Kochar Y, Lieuwen T, Seitzman J. Pressure and preheat dependence of laminar flame speeds of H_2/CO/CO_2/O_2/He mixtures. Proc Combust Inst 2009;32:1261–8.
[2] Park O, Veloo PS, Liu N, Egolfopoulos FN. Combustion characteristics of alternative gaseous fuels. Proc Combust Inst 2010;33:887–94.
[3] Sun H, Yang SI, Jomaas G, Law CK. High-pressure laminar flame speeds and kinetic modeling of carbon monoxide/hydrogen combustion. Proc Combust Inst 2007;31:439–46.
[4] Burke MP, Chaos M, Dryer FL, Ju Y. Negative pressure dependence of mass burning rates of H_2/CO/O_2/diluent flames at low flame temperatures. Combust Flame 2010;157:618–31.
[5] Bosschaart KJ, de Goey LPH. Detailed analysis of the heat flux method for measuring burning velocities. Combust Flame 2003;132:170–80.
[6] Krejci MC, Mathieu O, Vissotski AJ, Ravi S, Sikes TG, Peterson EL, et al. Laminar flame speed and ignition delay time data for the kinetic modeling of hydrogen and syngas fuel blends. J Eng Gas Turbines Power 2013;135:0215031–9.
[7] Kéromnès A, Metcalfe WK, Heufer KA, Donohoe N, Das AK, Sung C, et al. An experimental and detailed chemical kinetic modeling study of hydrogen and syngas mixture oxidation at elevated pressures. Combust Flame 2013;160:995–1011.
[8] Konnov AA. Remaining uncertainties in the kinetic mechanism of hydrogen combustion. Combust Flame 2008;152:507–28.
[9] Goswami M, Derks S, Coumans K, Slikker WJ, de Andrade Oliveira MH, Bastiaans RJM, et al. The effect of elevated pressures on the laminar burning velocity of methane + air mixtures. Combust Flame 2013;160:1627–35.
[10] Konnov AA, Puig Alvarez G, Rybitskaya IV, De Ruyck J. The effects of enrichment by carbon monoxide on adiabatic burning velocity and nitric oxide formation in methane flames. Combust Sci Technol 2009;181(1):117–35.
[11] de Goey LPH, Somers LMT, Bosch WMML, Mallens RMM. Modeling of the small scale structure of flat burner-stabilized flames. Combust Sci Technol 1995;104:387–400.
[12] McLean IC, Smith DB, Taylor SC. The use of carbon monoxide/hydrogen burning velocities to examine the rate of the CO + OH reaction. Proc Combust Inst 1994;25:749–57.
[13] Prathap C, Ray A, Ravi MR. Investigation of nitrogen dilution effects on the laminar burning velocity and flame stability of syngas fuel at atmospheric condition. Combust Flame 2008;155:145–60.
[14] Bouvet N, Chauveau C, Gokalp I, Halter F. Experimental studies of the fundamental flame speeds of syngas (H_2/CO)/air mixtures. Proc Combust Inst 2011;33:913–20.
[15] Galmiche B, Halter F, Foucher F, Dagaut P. Effects of dilution on laminar burning velocity of premixed methane/air flames. Energy Fuels 2011;25(3):948–54.
[17] Li J, Zhao Z, Kazakov A, Chaos M, Dryer FL. A comprehensive kinetic mechanism for CO, CH_2O and CH_3OH combustion. Int J Chem Kinet 2007;39(3):109–36.
[18] Somers LMT. The simulation of flat flames with detailed, reduced chemical models [PhD thesis]. Eindhoven University of Technology; 1994.
[19] Burcat A, Ruscic B. ANL-05/20 and TAE 960 Technion-IIT. Aerospace Engineering and Argonne National Laboratory Chemistry Division; 2005.
[20] Burke MP, Dryer FL, Ju Y. Assessment of kinetic modeling for lean H_2/CH_4/O_2/diluent flames at higher pressures. Proc Combust Inst 2011;33:905–12.
[21] Konnov AA. Implementation of the NCN pathway of prompt-NO formation in the detailed reaction mechanism. Combust Flame 2009;156:2093–105.
[22] Baulch DL, Bowman CT, Cobos CJ, Cox RA, Just T, Kerr JA, et al. Evaluated kinetic data for combustion modeling: supplement II. J Phys Chem Ref Data 2005;34(3):757–1397.
[23] Cohen N, Westberg KR. Chemical kinetic data sheets for high-temperature chemical reactions. J Phys Chem Ref Data 1983;12:531–90.
[24] Tsang W, Hampson RF. Chemical kinetic database for combustion chemistry. Part I. Methane and related compounds. J Phys Chem Ref Data 1986;15:1087–279.
[25] Sutherland JW, Michael JV, Pirraglia AN, Nesbitt FL, Klemm RB. Rate constant for the reaction of $O(_3P)$ with H_2 by the flash photolysis-shock tube and flash photolysis resonance fluorescence techniques; 504 K $\leq T \leq$ 2495 K. 21 Sym (Int) Combust – Combust Inst 1988;21(1):929–41.
[26] Hwang SM, Ryu SO, De Witt KJ, Rabinowitz MJ. High temperature rate coefficient measurements of H + O_2 chain-branching and chain-terminating reaction. Chem Phys Lett 2005;408:107–11.
[27] Hong Z, Davidson DF, Barbour EA, Hanson RK. A new shock tube study of the H + O_2 → OH + O reaction rate using tunable diode laser absorption of H_2O near 2.5 μm. Proc Combust Inst 2011;33:309–16.
[28] Mueller MA, Kim TJ, Yetter RA, Dryer FL. Flow reactor studies and kinetic modeling of the H_2/O_2 reaction. Int J Chem Kinet 1999;31:113–25.
[29] Troe J. Thermal dissociation and recombination of polyatomic molecules. 15 Sym (Int) Combust – Combust Inst 1975;15:667–80.
[30] Troe J, Gardiner Jr WC, editors. Combustion chemistry. New York: Springer-Verlag; 1984. pp. 171–96.
[31] Warnatz J, Gardiner Jr WC, editors. Combustion chemistry. New York: Springer-Verlag; 1984. p. 197.
[32] Westmoreland PR, Howard JB, Longwell JP, Dean AM. Prediction of rate constants and pyrolysis reactions by bimolecular QRRK. AIChE J 1986;32:1971–9.
[33] Allen MT, Yetter RA, Dryer FL. High pressure studies of moist carbon monoxide/nitrous oxide kinetics. Combust Flame 1997;109:449–70.
[34] Warnatz J, Maas U, Dibble RW. Combustion. Heidelberg: Springer-Verlag; 1996.
[35] Davis SG, Joshi AV, Wang H, Egolfopoulos FN. An optimized kinetic model of H_2/CO combustion. Proc Combust Inst 2005;30:1283–92.
[36] Troe J. Modeling the temperature and pressure dependence of the reaction HO + CO ⇌ HOCO ⇌ H + CO_2. 27 Sym (Int) Combust – Combust Inst 1998;27:167–75.
[37] Fulle D, Hamann HF, Hippler H, Troe J. High pressure range of addition reactions of HO. II. Temperature and pressure

dependence of the reaction HO + CO ⇔ HOCO → H + CO_2. J Chem Phys 1996;105:983–1000.
[38] Kim TJ, Yetter RA, Dryer FL. New results on moist CO oxidation: high pressure, high temperature experiments and comprehensive kinetic modeling. 25 Sym (Int) Combust – Combust Inst 1994;25:759–66.
[39] Sivaramakrishnan R, Comandini A, Tranter RS, Brezinsky K, Davis SG, Wang H. Combustion of CO/H_2 mixtures at elevated pressures. Proc Combust Inst 2007;31:429–37.
[40] Mittal G, Sung CJ, Fairweather M, Tomlin AS, Griffiths JF, Hughes KJ. Significance of the HO_2 + CO reaction during the combustion of CO + H_2 mixtures at high pressures. Proc Combust Inst 2007;31:419–27.
[41] Timonen RS, Ratajczk E, Gutman D. Kinetics of the reactions of the formyl radical with oxygen, nitrogen dioxide, chlorine and bromine. J Phys Chem 1988;92:651–5.
[42] Zhao Z, Li J, Kazakov A, Dryer FL. Temperature-dependent feature sensitivity analysis for combustion modeling. Int J Chem Kinet 2005;37:282–95.
[43] Baulch DL, Cobos CJ, Cox RA, Esser C, Frank P, Th Just, et al. Evaluated kinetic data for combustion modelling. J Phys Chem Ref Data 1992;21:411–735.
[44] Friedrichs G, Davidson DF, Hanson RK. Direct measurements of the reaction H + CH_2O → H_2 + HCO behind shock waves by means of vis–UV detection of formaldehyde. Int J Chem Kinet 2002;34:374–86.
[45] Larson CW, Stewart PH, Golden DM. Pressure and temperature dependence of reactions proceeding via a bound complex. An approach for combustion and atmospheric chemistry modelers. Application to HO + CO → [HOCO] → H + CO_2. Int J Chem Kinet 1988;20:27–40.
[46] Yu HG, Muckerman JT, Francisco JS. Direct ab initio dynamics study of the OH + HOCO reaction. J Phys Chem A 2005;109:5230–6.
[47] Miyoshi A, Matsui H, Washida N. Detection and reactions of the HOCO radical in gas phase. J Chem Phys 1994;100:3532–9.
[48] Petty JT, Harrison JA, Moore CB. Reactions of trans-HOCO studied by infrared spectroscopy. J Phys Chem 1993;97:11194–8.
[49] Nolte J, Grussdorf J, Temps F, Wagner HGg. Kinetics of the reaction of HOCO with O_2 in the gas phase. Z Naturforsch A 1993;48:1234–8.
[50] Poggi G, Francisco JS. An ab initio study of the competing reaction channels in the reaction of HOCO radicals with NO and O_2. J Chem Phys 2004;120:5073–80.
[51] Yu HG, Muckerman JT. Quantum molecular dynamics study of the reaction of O_2 with HOCO. J Phys Chem A 2006;110:5312–6.
[52] Tse SD, Zhu DL, Law CK. Morphology and burning rates of expanding spherical flames in H_2/O_2/inert mixtures up to 60 atmospheres. Proc Combust Inst 2000;28:1793–800.
[53] Kazakov A. Personal communication; 2004.
[54] Lutz AE, Kee RJ, Miller JA. Senkin: report SAND-87-8248. Albuquerque: Sandia National Laboratories; 1988.
[55] O'Connaire M, Curran HJ, Simmie JM, Pitz WJ, Westbrook CK. A comprehensive modeling study of hydrogen oxidation. Int J Chem Kinet 2004;36:603–22.
[56] Burke MP, Chaos M, Ju Y, Dryer FL, Klippenstein SJ. Comprehensive H_2/O_2 kinetic model for high-pressure combustion. Int J Chem Kinet 2012;44:444–74.
[57] Yetter RA, Dryer FL, Rabitz H. Flow reactor studies of carbon monoxide/hydrogen/oxygen kinetics. Combust Sci Technol 1991;79(1–3):129–40.
[58] Paletskii AA, Kuibida LV, Bolshova TA, Korobeinichev OP, Fristrom RM. Study of the structure of a tem-atmosphere H_2–O_2–Ar flame using molecular-beam inlet mass-spectrometric probing. Combust Explos Shock Waves 1996;32(3):245–50.
[59] Struckmeier U, Oßwald P, Kasper T, Böhling L, Heusing M, Kohler M, et al. Sampling probe influences on temperature and species concentrations in molecular beam mass spectroscopic investigations of flat premixed low-pressure flames. Z Phy Chem 2009;223(4–5):503–37.
[60] Naudet V, Javoy S, Paillard CE. A high temperature chemical kinetics study of the reaction: OH + Ar = H + O + Ar. Combust Sci Technol 2001;164:113–28.
[61] Troe J. Detailed modeling of the temperature and pressure dependence of the reaction H + O_2 (+M) → HO_2 (+M). Proc Combust Inst 2000;28:1463–9.
[62] Bates RW, Golden DM, Hanson RK, Bowman CT. Experimental study and modeling of the reaction H + O_2 + M → HO_2 + M (M = Ar, N_2, H_2O) at elevated pressures and temperatures between 1050 and 1250 K. Phys Chem Chem Phys 2001;3:2337–42.
[63] Atkinson R, Baulch DL, Cox RA, Hampson Jr RF, Kerr JA, Rossi MJ, et al. Evaluated kinetic and photochemical data for atmospheric chemistry: supplement VI. J Phys Chem Ref Data 1997;26:1329–799.
[64] Karkach SP, Osherov VI. Ab initio analysis of the transition states on the lowest triplet H_2O_2 potential surface. J Chem Phys 1999;110:11918–27.
[65] Kappel Ch, Luther K, Troe J. Shock wave study of the unimolecular dissociation of H_2O_2 in its falloff range and of its secondary reactions. Phys Chem Chem Phys 2002;4:4392–8.
[66] Atkinson R, Baulch DL, Cox RA, Crowley JN, Hampson RF, Hynes RG, et al. Evaluated kinetic and photochemical data for atmospheric chemistry: volume III – gas phase reactions of inorganic halogens. Atmos Chem Phys 2005;7:981–1191.
[67] Hippler H, Neunaber H, Troe J. Shock wave studies of the reactions HO + H_2O_2 → H_2O + HO_2 and HO + HO_2 → H_2O + O_2 between 930 and 1680 K. J Chem Phys 1995;103:3510–6.